Systematic Evaluation and Analysis for 60-GHz Dielectric Resonators Coupled to a Microstrip Line on a GaAs Substrate

Ken'ichi Hosoya, Takashi Inoue, Masahiro Funabashi, and Keiichi Ohata, *Member, IEEE*

***Abstract*— This paper presents the first systematic evaluation and analysis of 60-GHz-band $\mathrm{TE}_{01\delta}$-mode cylindrical dielectric resonators coupled to a microstrip line on a GaAs substrate. The loss components of the unloaded Q are analyzed using simple numerical techniques. The distance between the resonator center and the microstrip line which gives the maximum coupling coefficient is found to be approximately 3/5 of the resonator radius, whose ratio is almost constant for all practical cases. The temperature characteristics are also demonstrated and the origins of temperature dependences of the unloaded Q and the coupling coefficient are discussed. An equivalent circuit model for the dielectric resonator coupled to the microstrip line is presented, whose element parameters can express the dependences of the resonant frequency, the unloaded Q, and the coupling coefficient on the structural parameters and the temperature.**

***Index Terms*— Dielectric resonators, electromagnetic coupling, equivalent circuits, MMIC's, microstrip, Q factor.**

I. Introduction

DIELECTRIC resonators coupled to a microstrip line have been used in microwave circuits such as dielectric resonator oscillators (DRO's), filters, etc. [1]. In recent years, there has been a growing interest in the development of millimeter-wave application systems [2]. For example, V-band monolithic microwave integrated circuit (MMIC) DRO's have been reported by several authors [3]–[5]. In those monolithic circuits, GaAs heterojunction field-effect transistors are employed as an active device and dielectric resonators are placed directly on the same MMIC chip to avoid the use of bonding wires which are lossy and difficult to characterize in the millimeter-wave range. $\mathrm{TE}_{01\delta}$ fundamental-mode cylindrical resonators are adopted because of their small diameters compared with Whispering-Gallery-mode resonators which have been used in millimeter-wave hybrid integrated circuit (HIC) oscillators [6]. For the design of such DRO's in the millimeter-wave frequency range, accurate characterization of a dielectric resonator coupled to a microstrip line on a GaAs substrate is necessary. A large number of experimental studies [7], [8] and theoretical studies [9]–[14] have been reported to characterize the $\mathrm{TE}_{01\delta}$ dielectric resonator coupled to the microstrip line. However, most of these works were done in the microwave range and the resonators were placed on an alumina or Teflon substrate for HIC applications.

This paper presents the systematic evaluation and analysis for a 60-GHz-band $\mathrm{TE}_{01\delta}$-mode $\mathrm{Ba(Mg,Ta)O_3}$ cylindrical dielectric resonator coupled to a microstrip line fabricated on a GaAs substrate with the object of millimeter-wave monolithic circuit applications. The loss components of the unloaded Q are analyzed using simple numerical techniques [9], [10]. The maximum coupling coefficient was found when the distance between the resonator center and the microstrip line was approximately 3/5 of the resonator radius. It is shown by a theoretical calculation using the magnetic-flux method [14] that this ratio is almost constant for all practical cases. The temperature characteristics of the resonant frequency, the unloaded Q, and the coupling coefficient are also shown, which are necessary for stability design of DRO's [15]. Using the results above, an equivalent circuit model for the dielectric resonator coupled to the microstrip line is derived, whose element parameters depend on the airgap between the resonator top surface and a tuning screw, the distance between the resonator and the microstrip line, and the temperature.

II. Experiment

For designing DRO's and filters, we have to know the values of the resonant frequency, the unloaded Q, and the coupling coefficient of the dielectric resonator placed in the same environment, as is used in the circuits. In this study, we coupled a dielectric resonator to a microstrip line on a GaAs substrate and extracted those values from measured S-parameters by a procedure described as follows.

A. Experimental Setup

Measurement was performed on a cylindrical dielectric resonator of diameter 1.3 mm and height 0.55 mm, made of $\mathrm{Ba(Mg,Ta)O_3}$ whose relative dielectric constant ε_r is 23.8. The resonator is placed on top of a dielectric substrate mounted on a test fixture with a tuning screw, as shown in Fig. 1(a). The substrate is made of 40-μm-thick semi-insulating GaAs (relative dielectric constant ε_{rs} is 12.6) with a ground metal (Au) on the underside. Fig. 1(b) shows the configuration of the substrate surface. A 6.6-mm-long center conductor of 30-μm width and the ground pads for on-wafer measurement with G–S–G probes are fabricated on the substrate surface. Via holes of 30-μm-square are formed to connect the ground pads

Manuscript received April 3, 1997; revised January 14, 1998.

K. Hosoya, T. Inoue, and K. Ohata are with Kansai Electronics Research Laboratory, NEC Corporation, Otsu, Shiga 520, Japan.

M. Funabashi is with C&C LSI Development Division, NEC Corporation, Nakahara-ku, Kawasaki 221, Japan.

Publisher Item Identifier S 0018-9480(98)02728-8.

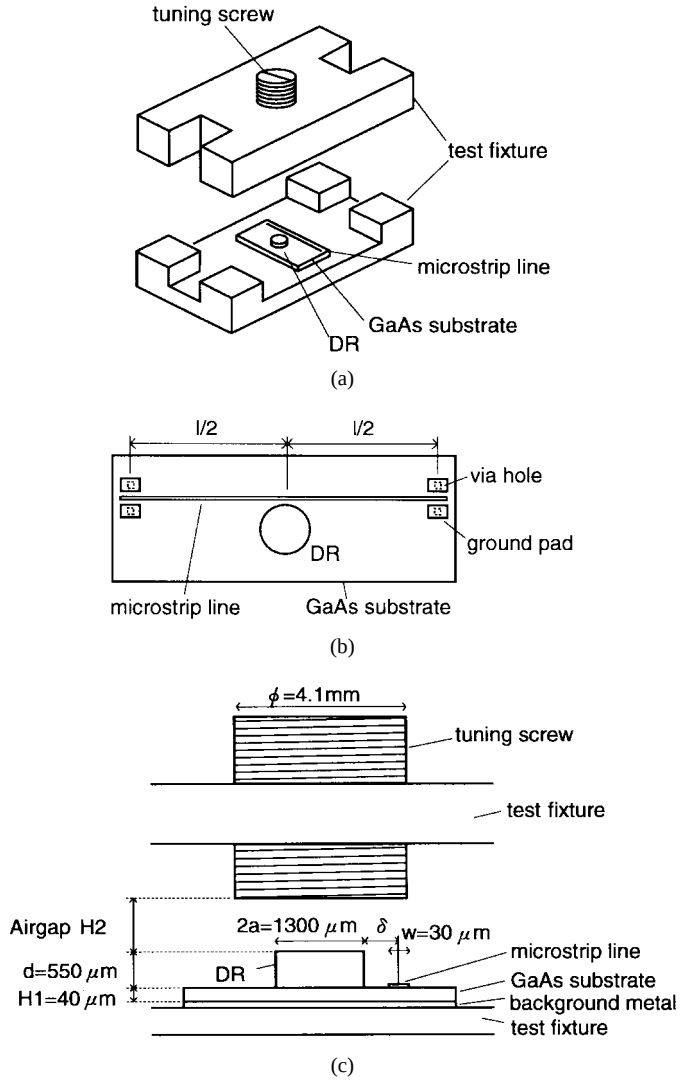

Fig. 1. Measurement setup. (a) Test fixture. (b) Configuration of a substrate surface. (c) Cross-sectional view of a resonant structure.

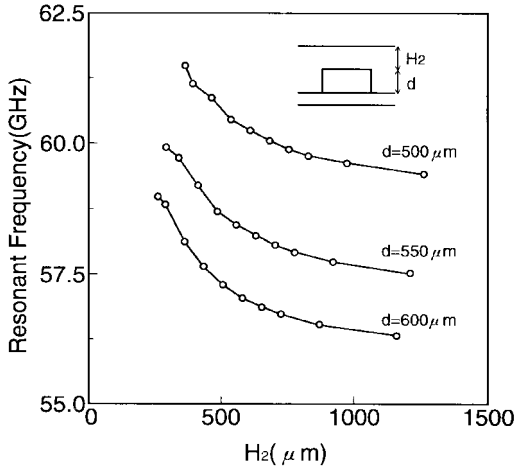

Fig. 2. Resonant frequency versus the airgap for the various resonator thickness.

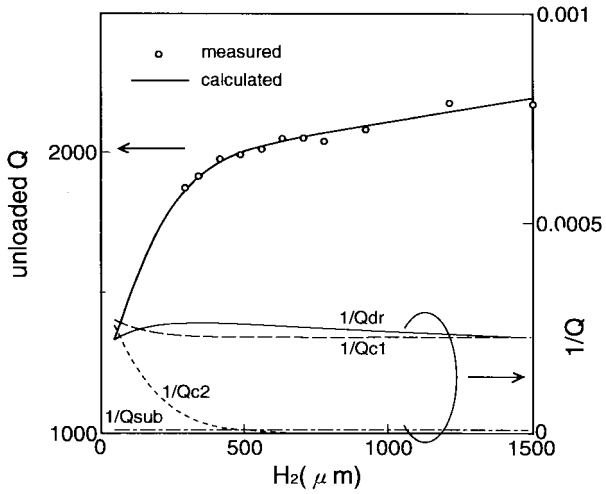

Fig. 3. Unloaded Q versus the airgap for $\delta = -200$ μm. The following constants are used in the calculation: the conductivity of the lower and upper plate, $\sigma = 43 \times 10^6$ S/m, the dielectric loss tangent of the resonator and the substrate, $\tan\delta_{dr} = 3.3f \times 10^{-6}, \tan\delta_{\rm sub} = 1.6 \times 10^{-4}$, where f is the frequency in gigahertz.

to the ground metal. Fig. 1(c) shows the cross-sectional view of the resonant structure. The airgap H_2 is variable over the range from 290 to 1500 μm by rotating the tuning screw.

B. Experimental Procedure and Data Processing

The two-port scattering matrix was measured around the resonant frequency by a network analyzer integrated with an on-wafer probe station. However, the measured S-matrix $[S_{\rm measured}]$ includes the effects of the transmission loss and of the impedance mismatch at the end of the microstrip line. The corresponding F-matrix without these effects can be expressed as follows:

$$[F]_0 = [F_{\rm MSL}]^{-1}[F_{\rm measured}][F_{\rm MSL}]^{-1} \quad (1)$$

where $[F_{\rm measured}]$ is the F-matrix converted from $[S_{\rm measured}]$ and $[F_{\rm MSL}]$ is the F-matrix of the microstrip line of length l/2. The characteristic impedance and the propagation constant included in $[F_{\rm MSL}]$ were determined using the direct transmission method [16]. $[F]_0$ expresses the effect of dielectric resonator on the transmission characteristics of the microstrip line [13]. Finally, the unloaded Q and the coupling coefficient were calculated from $[F]_0$ using the reaction method, such as described by Podcameni *et al.* [7].

III. Result and Discussion

A. Resonant Frequency and Unloaded Q

The resonant frequency and unloaded $Q(Q_u)$ were measured as airgap H_2 was varied by rotating the tuning screw for a constant $\delta, \delta_0 = -200$ μm. The experimental resonant frequency as a function of H_2 is shown in Fig. 2. The results for the resonators of $d = 500$ μm and 600 μm are also shown in the figure. This shows that the resonant frequencies can be varied over a 2-GHz range.

The measured unloaded Q as a function of H_2 is plotted in Fig. 3 by open dots. As shown in Fig. 3, Q_u increases rapidly with H_2 when H_2 is below 410 μm, while Q_u increases slowly with H_2 when H_2 is above 410 μm. The measured

Q_u (~2000) is lower than the Q-factor of the resonator itself (~5000), because the electromagnetic losses of other components degrade Q_u.

Analysis of loss components was performed by numerical calculation. If we assume that the tuning screw and the substrate are of infinite extent, the unloaded Q can be expressed as

$$\frac{1}{Q_u} = \frac{1}{Q_{dr}} + \frac{1}{Q_{\text{sub}}} + \frac{1}{Q_{c1}} + \frac{1}{Q_{c2}} \tag{2}$$

where Q_{dr}, Q_{sub}, Q_{c1}, and Q_{c2} are Q-factors due to the dielectric loss of the resonator, the dielectric loss of the substrate, the conductor loss of the lower plate, and the conductor loss of the upper plate, respectively. Each Q-factor Q_j $(j = dr,\ \text{sub},\ c1, c2)$ was calculated using the techniques presented by Mongia and Bhartia [9] and Dydyk [10]. The resonant frequency and electromagnetic fields required for Q_j calculations were determined by the dielectric waveguide model (DWM) method [11].

A theoretical curve of Q_u calculated by (2) is shown in Fig. 3 by a solid line. Theoretical curves of $1/Q_j$ $(j = dr,\ \text{sub},\ c1, c2)$ are also shown in Fig. 3 by solid and dashed lines on the right axis. These curves show that the rapid increase of Q_u with increase in H_2 for $H_2 \leq 410$ μm $(\equiv H_{2_1})$ is due to the increase of the upper plate Q-factor Q_{c2}. For $H_2 \geq H_{2_1}$, $1/Q_{c2}$ and $1/Q_{\text{sub}}$ become negligibly small, and $1/Q_{dr}$ and $1/Q_{c1}$ are primal factors in the degradation of Q_u. Therefore, it should be possible to increase Q_u effectively by increasing the substrate thickness and thus Q_{c1}.

In the above calculation, we assumed that the radiation loss due to the absence of the sidewall is negligibly small because the tuning screw has a sufficiently large area (the screw diameter is over three times the resonator diameter). Good agreement between the experimental result and calculation confirms the validity of this assumption.

B. Coupling Coefficient

Some experimental studies [8] have been reported to characterize coupling between a dielectric resonator and a microstrip line. In those studies, the dielectric resonator was placed adjacent to the microstrip center conductor, which is the range of $\delta \geq 0$. However, in the millimeter-wave range where the conductor and dielectric losses are large, and consequently Q_u is very small, there are cases where the resonator must be laid on the center conductor of the microstrip line (i.e., $\delta \leq 0$) to achieve sufficient coupling coefficient.

The coupling coefficient was measured as δ was varied in the range from -650 μm $(= -a)$ to 200 μm for a constant airgap $H_{2_0} = 290$ μm. The experimental coupling coefficient β as a function of δ is shown in Fig. 4 by open dots. The maximum β was found at about $\delta = -250$ μm (approximately 0.4 times the resonator radius a). These results were verified numerically by the theoretical curve shown in Fig. 4 using the polarization current [12] where the electric fields in the microstrip line were calculated by the finite-difference method assuming the sidewall sufficiently far from the resonator. The calculated result indicated by the solid line shows good agreement with the experimental one.

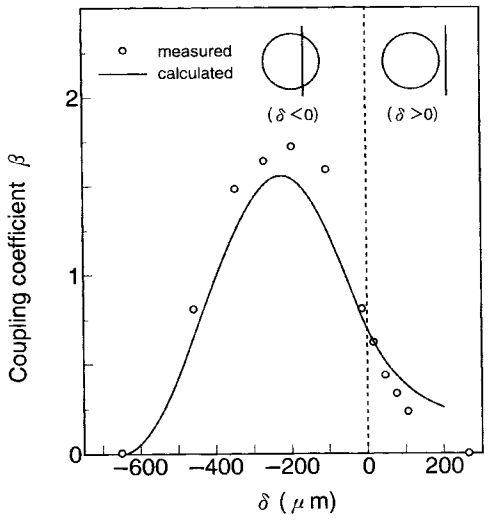

Fig. 4. Coupling coefficient versus the distance between the resonator and the microstrip line for $H_2 = 290$ μm.

Here, we discuss an interesting parameter δ_m defined as δ which gives the maximum coupling coefficient β. The values of δ_m/a were calculated while changing the structural parameters $(d/a, H_1/a, H_2/a)$ normalized by the resonator radius a and dielectric constants of the resonator and the substrate $(\varepsilon_r, \varepsilon_{rs})$. In the calculation, we used the magnetic-flux method [14] instead of the time-consuming polarization current method. Applying the magnetic-flux method to the range of $\delta \leq 0$, the following expression for the coupling coefficient can be obtained:

$$\beta = \frac{\omega_0 \mu_0^2 Q_u}{4 Z_0 W_e} \left\{ \iint_S \vec{H} \cdot d\vec{S} \right\}^2 \tag{3}$$

where

$$\iint_S \vec{H} \cdot d\vec{S} = -2(a+\delta)\sinh\beta_2 H_1 \left\{ \int_0^{x_a} \frac{J_1(h_1 r)}{h_1 r}\, dx - \frac{J_0(h_1 a)}{K_0(h_4 a)} \cdot \int_{x_a}^{\infty} \frac{K_1(h_4 r)}{h_4 r}\, dx \right\} \tag{4}$$

where $\vec{H}$ is the magnetic component in the substrate, S denotes the section between the microstrip line and the bottom conductor [14], and W_e is the electric energy in the resonant structure. $J_n(\cdot)$ and $K_n(\cdot)$ are the first-kind Bessel function of nth order and the modified second-kind Bessel function of nth order, respectively. The lengths r and x_a are defined as $r = \sqrt{(a+\delta)^2 + x^2}, x_a = \sqrt{a^2 - (a+\delta)^2}$, respectively. h_1, h_4 (the radial wavenumbers inside and outside of the resonator), and β_2 (the vertical wavenumber in the substrate) were calculated by the DWM method. Fig. 5 shows the dependences of δ_m/a on structural parameters calculated using (3) and (4). The dependence of δ_m/a on the dielectric constants is not shown in this paper because it is almost independent of $\varepsilon_r, \varepsilon_{rs}$. The values of δ_m/a were found to be

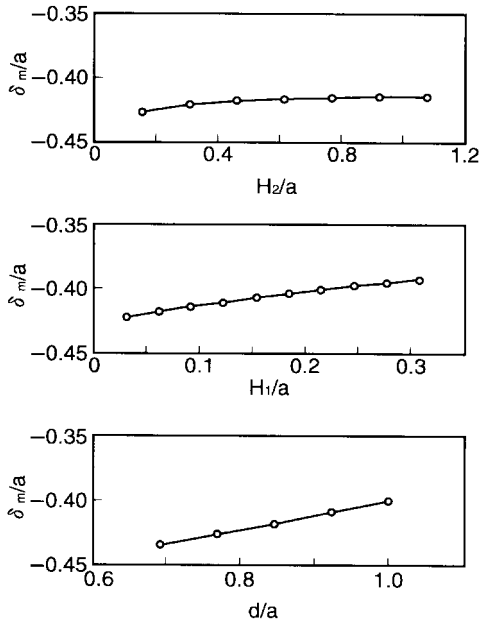

Fig. 5. Structural parameters dependences of δ_m/a calculated by magnetic-flux method.

within the range from -0.44 to -0.39 when the structural parameters were changed individually over a wide range, which includes almost all practical cases. These results show that the coupling coefficient β becomes maximum when δ is about $-0.4a$ regardless of the structural parameters, dielectric constants, and consequently, resonant frequencies. From the viewpoint of electromagnetic-field distribution, it can be said that the horizontal magnetic-field components of the $\mathrm{TE}_{01\delta}$-mode resonator under the microstrip line, which induce the voltage on microstrip line, become maximum when δ is around $-0.4a$ regardless of these structural parameters.

C. Temperature Dependence

The dependences of the resonant frequency, the unloaded Q, and the coupling coefficient on the temperature were examined in the range from 0°C to 50°C for $H_{2_0} = 290\ \mu$m, $\delta_0 = -200\ \mu$m.

Fig. 6(a) shows the temperature characteristics of the resonant frequency. The plots are almost linear within this temperature range and the temperature coefficient of the resonant frequency is 9.4 ppm/°C. This value is considerably higher than that of the dielectric resonator itself (4.1 ppm/°C). This is probably due to the fact that the expansion or contraction of the test fixture and the substrate, and the relative dielectric constant variation of the substrate have more effect on the temperature coefficient than those of a dielectric resonator itself.

The temperature characteristics of the unloaded Q and the coupling coefficient are shown in Fig. 6(b) and (c). Both of them decrease almost linearly with increasing temperature in this temperature range. The slopes are $(\Delta Q_u/\Delta T)_{H_{2_0},\delta_0} = -9.7/$°C and $(\Delta\beta/\Delta T)_{H_{2_0},\delta_0} = -5.6\times10^{-3}/$°C.

For $H_2 = H_{2_0}$, Q_u can be approximated as

$$\frac{1}{Q_u} \simeq \frac{1}{Q_{dr}} + \frac{1}{Q_{c1}} \tag{5}$$

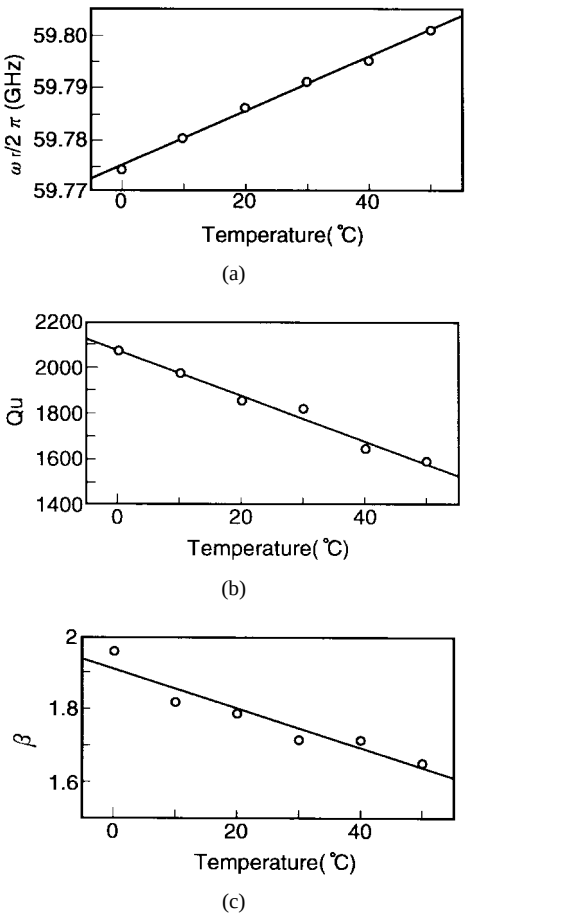

Fig. 6. Temperature dependences of (a) resonant frequency, (b) unloaded Q, and (c) coupling coefficient for $H_2 = 290\ \mu$m, $\delta = -200\ \mu$m. Solid lines were drawn by the least squares method.

(see Fig. 3). As a rule, $1/Q_{c1}$ is proportional to a square root of the resistivity of the ground metal [9], and $1/Q_{dr}$ is proportional to the dielectric loss tangent of the resonator. If we assume the dielectric loss tangent is proportional to the absolute temperature [17] and use the reported value of temperature coefficient for the resistivity of the ground metal (Au), we can explain a decrease in the measured Q_u of approximately 300 in the temperature range from 0 °C to 50 °C using (5), in good agreement with Fig. 6(b). This indicates that main factors which determine the slope of Q_u are the temperature dependences of the resistivity of the ground metal and the dielectric loss tangent of the resonator. The coupling coefficient β can be expressed as $\beta = Q_u/Q_{\mathrm{ext}}$ where Q_{ext} is the external Q-factor. Q_{ext} depends on only electromagnetic-field distribution, not on conductivities and dielectric loss tangents in the first-order approximation. Therefore, the slope of β can be regarded as the result of the temperature dependence of Q_u, i.e.,

$$\left(\frac{\Delta\beta}{\Delta T}\right)_{H_{2_0},\delta_0} \simeq \frac{1}{Q_{\mathrm{ext}}}\left(\frac{\Delta Q_u}{\Delta T}\right)_{H_{2_0},\delta_0}. \tag{6}$$

This approximation is confirmed by the fact that $(\Delta\beta/\Delta T)_{H_{2_0},\delta_0}$ calculated by (6) is $-8.8\times10^{-3}/$°C, which is close to the measured value $(-5.6\times10^{-3}/$°C).

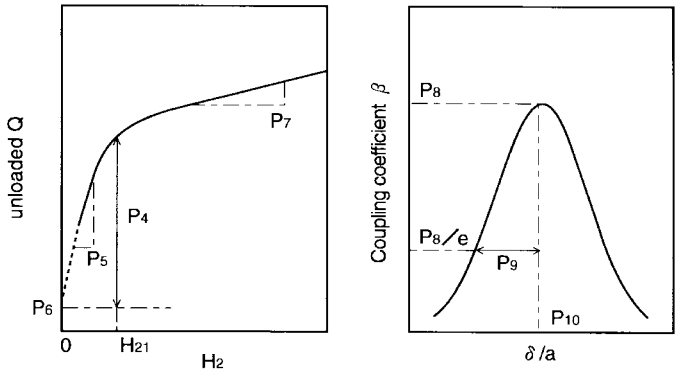

Fig. 7. Schematic representation of parameters $P_i (i = 4 \sim 10)$.

TABLE I
PARAMETERS INCLUDED IN (10)–(12)

P_1	$8.16 \times 10^{12} (rad \cdot m/sec)$	P_6	1.1×10^3
P_2	$-5.8 \times 10^{-5} (m)$	P_7	$0.2 \times 10^6 (m^{-1})$
P_3	$3.52 \times 10^{11} (rad/sec)$	P_8	1.75
P_4	8.0×10^2	P_9	0.397
P_5	$5.0 \times 10^3 (m^{-1})$	P_{10}	−0.35

D. Equivalent Circuit Model

For the design of dielectric-resonator circuits like DRO's and filters, it is very convenient to use an equivalent circuit model for a dielectric resonator coupled to a microstrip line. Using the experimental and numerical results described above, an equivalent circuit model was derived whose element parameters depend on the airgap H_2, the distance δ between the dielectric resonator and the microstrip line, and the temperature T. The two-port network having F-matrix $[F]_0$ can be expressed as a series high-Q parallel resonant circuit [7]. The parallel resonant-circuit parameters R, L, and C were determined based on the following assumptions which were approximately consistent with the experimental results.

1) The resonant angular frequency ω_r and the unloaded Q, Q_u are independent of δ.
2) The coupling coefficient β is independent of H_2.

Based on these assumptions, the parallel resonant-circuit parameters can be written as follows:

$$R = 2Z_0 \beta(\delta, T) \tag{7}$$

$$L = \frac{2Z_0 \beta(\delta, T)}{\omega_r(H_2, T) Q_u(H_2, T)} \tag{8}$$

$$C = \frac{Q_u(H_2, T)}{2Z_0 \omega_r(H_2, T) \beta(\delta, T)} \tag{9}$$

where Z_0 is the impedance of the measurement system. The forms of the unknown functions $\omega_r(H_2, T)$, $Q_u(H_2, T)$, and $\beta(\delta, T)$ were chosen to be consistent with the experimental results using appropriate simple analytical functions as follows:

$$\omega_r(H_2, T) = \frac{P_1}{H_2 - P_2} + P_3 + \left(\frac{\Delta \omega_r}{\Delta T}\right)_{H_2 = H_{2_0}} (T - T_0) \tag{10}$$

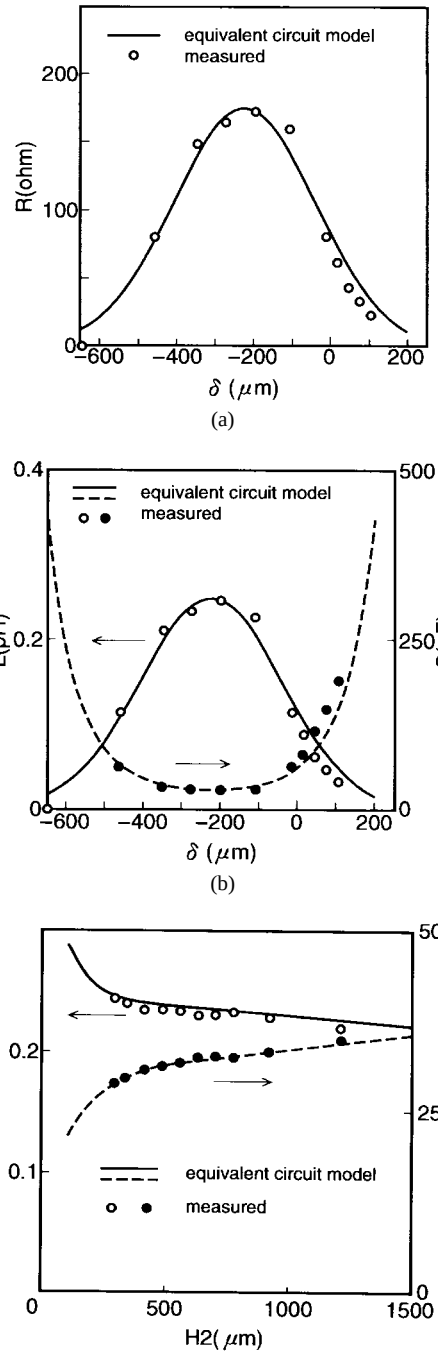

Fig. 8. Structural parameter dependences of equivalent circuit parameters for constant temperature $T = T_0$. (a) Resistance as a function of δ for $H_2 = 290$ μm. (b) Inductance and capacitance as functions of δ for $H_2 = 290$ μm. (c) Inductance and capacitance as functions of H_2 for $\delta = -200$ μm.

$$Q_u(H_2, T) = P_4 \tanh(P_5 H_2) + P_6 + P_7 H_2 + \left(\frac{\Delta Q_u}{\Delta T}\right)_{H_2 = H_{2_0}} (T - T_0) \tag{11}$$

$$\beta(\delta, T) = \left\{ \left(\frac{\Delta \beta}{\Delta T}\right)_{\delta = \delta_0} (T - T_0) + P_8 \right\} \cdot \exp\left\{ -\frac{1}{P_9^2} \left(\frac{\delta}{a} - P_{10}\right)^2 \right\} \tag{12}$$

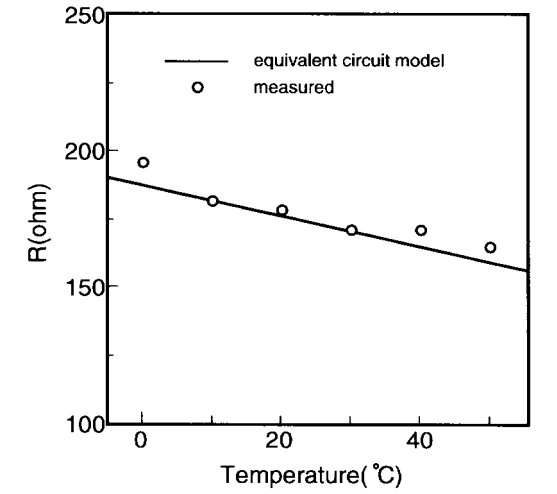

(a)

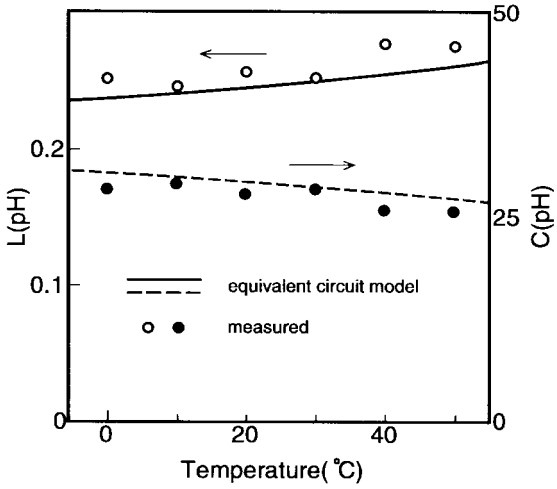

(b)

Fig. 9. Temperature dependences of equivalent circuit parameters for constant structural parameters $H_2 = H_{2_0}$, $\delta = \delta_0$. (a) Resistance. (b) Inductance and capacitance.

where

P_1, P_2, P_3	parameters to represent $\omega_r(H_2)$ by hyperbola;
P_4	difference between $Q_u(H_2 = H_{2_1})$ and $Q_u(H_2 \to 0)$;
P_5	slope of the function $Q_u(H_2)$ in the linear region for $H_2 \leq H_{2_1}$;
P_6	value of Q_u for $H_2 \to 0, T = T_0$;
P_7	slope of the function $Q_u(H_2)$ in the linear region for $H_2 \geq H_{2_1}$;
P_8	maximum β as a function of δ for $T = T_0$;
P_9	difference between δ_m/a and δ_1/a, where $\beta(\delta_m) = P_8, \beta(\delta_1) = P_8/e$ for $T = T_0$ (e is the base of natural logarithm);
P_{10}	δ/a which gives maximum $\beta(= \delta_m/a)$.

Meanings of parameters $P_i (i = 4 \sim 10)$ are described schematically in Fig. 7. Determined values of $P_i (i = 1 \sim 10)$ are shown in Table I. The values of temperature coefficients $(\Delta\omega_r/\Delta T)_{H_2=H_{2_0}}$, $(\Delta Q_u/\Delta T)_{H_2=H_{2_0}}$, and $(\Delta\beta/\Delta T)_{\delta=\delta_0}$ were described in the previous subsection. The dependences of the equivalent circuit parameters R, L, and C on the structural parameters and the temperature calculated using (7)–(12) are shown by solid and dashed lines in Fig. 8(a)–(c) and Fig. 9(a) and (b). The equivalent circuit parameters deduced from measured ω_r, Q_u, and β are also shown in Figs. 8 and 9 by open and closed dots. These results indicate that equations (7)–(12) are adequate approximations of the measured data. The parameters P_i must be extracted if dimensions and dielectric constants of the resonator and the substrate are changed, but the selected functions contained in (10)–(12) are valid for almost all practical cases. Equations (7)–(12) are easily put in the commercially available microwave computer-aided design (CAD) programs and make it possible to analyze the dependences of the dielectric-resonator circuit performances such as the oscillation frequency and output power of DRO's on structural parameters and the temperature.

IV. Conclusions

Systematic evaluation results for the 60-GHz-band $TE_{01\delta}$-mode $Ba(Mg,Ta)O_3$ cylindrical dielectric resonators coupled to a microstrip line have been presented. The loss components of unloaded Q were discussed using the simple calculation method. The maximum coupling coefficient was found when the distance between the resonator center and the microstrip line was approximately 3/5 of the resonator radius. It was shown by numerical calculation that this distance is almost independent of structural parameters. The temperature characteristics were also demonstrated and the origins of temperature dependences of the unloaded Q and the coupling coefficient were discussed. Furthermore, an equivalent circuit model for the dielectric resonator coupled to the microstrip line was presented, whose element parameters depend on the airgap, the distance between the resonator and the microstrip line, and the temperature.

Acknowledgment

The authors wish to thank H. Nagai for his cooperation in microwave measurement and Dr. H. Abe, Dr. M. Ogawa, and Dr. M. Kuzuhara for their constant encouragement.

References

[1] J. K. Plourde and C.-L. Ren, "Application of dielectric resonator in microwave components," *IEEE Trans. Microwave Theory Tech.*, vol. MTT-29, pp. 754–770, Aug. 1981.

[2] Y. Takimoto and T. Ihara, "Research activities on millimeter wave indoor communication systems in Japan," in *1993 IEEE MTT-S Microwave Symp. Dig.*, Atlanta, GA, June 1993, pp. 673–676.

[3] M. Funabashi, K. Ohata, K. Onda, K. Hosoya, T. Inoue, M. Kuzuhara, K. Kanekawa, and Y. Kobayashi, "A V-band AlGaAs/InGaAs heterojunction FET MMIC dielectric resonator oscillator," in *IEEE GaAs IC Symp. Dig.*, Philadelphia, PA, Oct. 1994, pp. 30–33.

[4] T. Inoue, K. Ohata, M. Funabashi, K. Hosoya, M. Maruhashi, Y. Makino, and M. Kuzuhara, "60 GHz dielectrically stabilized monolithic voltage controlled oscillator," in *Proc. 25th European Microwave Conf.*, Bologna, Italy, Sept. 1995, pp. 281–284.

[5] U. Güttich and J. Wenger, "Design, fabrication and performance of monolithic dielectrically stabilized PM-HEMT oscillators up to 60

GHz," in *Proc. 24th European Microwave Conf.*, Cannes, France, Sept. 1994, pp. 361–365.
[6] D. Cros, C. Tronche, P. Guillon, and B. Theron, "W-band whispering gallery dielectric resonator mode oscillator," *IEEE MTT-S Microwave Symp. Dig.*, Boston, MA, June 1991, pp. 929–932.
[7] A. Podcameni, L. F. M. Conrado, and M. M. Mosso, "Unloaded quality factor measurement for MIC dielectric resonator applications," *Electron. Lett.*, vol. 17, no. 18, pp. 656–658, Sept. 1981.
[8] D. Kajfez and J. Guo, "Precision measurement of coupling between microstrip and $\mathrm{TE}_{01\delta}$ mode dielectric resonator," *Electron. Lett.*, vol. 30, no. 21, pp. 1771–1772, Oct. 1994.
[9] R. K. Mongia and P. Bhartia, "Accurate conductor Q-factor of dielectric resonator placed in an MIC environment," *IEEE Trans. Microwave Theory Tech.*, vol. 41, pp. 445–449, Mar. 1993.
[10] M. Dydyk, "Dielectric resonators add Q to MIC filters," *Microwaves*, vol. 16, no. 12, pp. 150–160, Dec. 1977.
[11] T. Itoh and R. S. Rudokas, "New method for computing the resonant frequencies of dielectric resonators," *IEEE Trans. Microwave Theory Tech.*, vol. MTT-25, pp. 52–54, Jan. 1977.
[12] P. Skalicky, "Coupling coefficient between dielectric resonator and microstrip line," *Electron. Lett.*, vol. 17, no. 2, pp. 99–100, Jan. 1981.
[13] Y. Komatsu and Y. Murakami, "Coupling coefficient between microstrip line and dielectric resonator," *IEEE Trans. Microwave Theory Tech.*, vol. MTT-31, pp. 34–40, Jan. 1983.
[14] P. Guillon, B. Byzery, and M. Chaubet, "Coupling parameters between a dielectric resonator and a microstripline," *IEEE Trans. Microwave Theory Tech.*, vol. MTT-33, pp. 222–226, Jan. 1985.
[15] C. Tsironis and V. Pauker, "Temperature stabilization of GaAs MESFET oscillators using dielectric resonators," *IEEE Trans. Microwave Theory Tech.*, vol. MTT-31, pp. 312–314, Mar. 1983.
[16] Y.-C. Shih, "Broad-band characterization of conductor-backed coplanar waveguide using accurate on-wafer measurement techniques," *Microwave J.*, pp. 95–105, Apr. 1991.
[17] H. Tamura, "Microwave dielectric materials," *MWE'92 Microwave Workshop Dig.*, Tokyo, Japan, 1992, pp. 77–85.

Ken'ichi Hosoya was born in Kanagawa, Japan, on October 15, 1966. He received the B.A. degree in pure and applied science from the University of Tokyo, Tokyo, Japan, in 1991.

In 1991, he joined NEC Corporation, Shiga, Japan, where he has been engaged in the development of millimeter-wave heterojunction FET's and MMIC's, such as power amplifiers and DRO's. His current research interest includes design and analysis of nonlinear microwave and millimeter-wave circuits.

Mr. Hosoya is a member of the Institute of Electronics, Information and Communication Engineers (IEICE), Japan.

Takashi Inoue received the B.S. degree in synthetic chemistry, the B.E. degree in applied mathematics and physics, and the M.E. degree in molecular engineering from Kyoto University, Kyoto, Japan, in 1983, 1985, and 1987, respectively.

In 1987, he joined NEC Corporation where he has been engaged in superconducting devices. Since 1992, he has been working on millimeter-wave MMIC's. He is currently an Assistant Manager with Kansai Electronics Research Laboratory, Shiga, Japan.

Mr. Inoue is a member of the Institute of Electronics, Information and Communication Engineers (IEICE), Japan.

Masahiro Funabashi received the B.S. degree in electrical engineering from Saitama University, Saitama, Japan, in 1980.

In 1980, he joined NEC Corporation, Yokohama, Japan, where he has been engaged in development of microwave integrated circuits. From July 1991 to March 1996, he was with Advanced Millimeter-Wave Technologies, Otsu, Japan. He is currently an Engineering Manager with C&C LSI Development Division, NEC Corporation, Kawasaki, Japan. His current interest includes millimeter-wave monolithic-integrated-circuits-based heterojunction transistors.

Mr. Funabashi is a member of the Institute of Electronics, Information and Communication Engineers (IEICE), Japan.

Keiichi Ohata (M'86) received the B.E. and M.E. degrees in electronic engineering from Kyoto University, Kyoto, Japan, in 1970 and 1972, respectively.

In 1972, he joined the Central Research Laboratories, NEC Corporation, Kawasaki, Japan, where he was engaged in the research of ohmic contacts to GaAs, development of low-noise GaAs MESFET's, and research and development of microwave and millimeter-wave heterojunction devices. From April 1991 to March 1996, he was temporarily transferred to Advanced Millimeter Wave Technologies, Otsu, Japan, where he was responsible for the research of 60-GHz-band MMIC's for short-range communication systems. He is currently a Senior Principal Researcher with Kansai Electronics Research Laboratory, NEC Corporation, Shiga, Japan, where he conducts research and development on millimeter-wave devices for multimedia communications.

Mr. Ohata is a member of the IEEE Microwave Theory and Techniques Society, IEEE Electron Devices Society, Institute of Electronics, Information and Communication Engineers (IEICE), Japan, and Japan Society of Applied Physics.